Preclinical Pharmacologic Evaluation of Pralatrexate and Romidepsin Confirms Potent Synergy of the Combination in a Murine Model of Human T-cell Lymphoma

Salvia Jain[1], Xavier Jirau-Serrano[2], Kelly Zullo[2], Luigi Scotto[2], Carmine F Palermo[3,4], Stephen A. Sastra[3,4,7], Kenneth P. Olive[3,4,7], Serge Cremers[3,4] , Tiffany Thomas[3], Ying Wei[5], Yuan Zhang[5], Govind Bhagat[3,], Jennifer Amengual[2], Changchun Deng[2], Charles Karan[6], Ronald Realubit[6], Susan Bates,

Owen A. O'Connor[2*]

[1]Beth Israel Deaconess Medical Center, Harvard Medical School, Boston, MA; [2]Center for Lymphoid Malignancies; [3]Department of Pathology and Cell Biology, [4]Department of Medicine, [5]Department of Biostatistics, [6] Department of Systems Biology High-Throughput Screening Facility, [7]Herbert Irving Comprehensive Cancer Center, Columbia University Medical Center, New York, NY

Running Title: Pralatrexate and romidepsin in preclinical T-cell lymphoma

Keywords: T-cell lymphoma, surface bioluminescence, three-dimensional ultrasound, romidepsin, pralatrexate

∗ Corresponding Author
All correspondence should be addressed to:
Owen A. O'Connor, M.D., Ph.D.
Professor of Medicine and Experimental Therapeutics
Director of the Center for Lymphoid Malignancies
Columbia University Medical Center
New York, NY 10019
Phone: 212-326-5720
Fax: 212-326-5725
E-mail: owenoconnor@cumc.columbia.edu

Conflicts of Interest: Dr. Owen A. O'Connor: research support from Spectrum Pharmaceuticals and Celgene. All other authors have no conflicts of interest.

Abstract

Purpose: T-cell lymphomas (TCLs) are aggressive diseases, which carry a poor prognosis. The emergence of new drugs for TCL has created a need to survey these agents in a rapid and reproducible fashion, in order to prioritize combinations which should be prioritized for clinical study. Mouse models of TCL that can be used for screening novel agents and their combinations are lacking. Developments in non-invasive imaging modalities like surface bioluminescence (SBL) and 3-dimensional-ultrasound are challenging conventional approaches in xenograft modeling relying on caliper measurements. The recent approval of pralatrexate and romidepsin creates an obvious combination that could produce meaningful activity in TCL, which has yet to be studied in combination.

Experimental Design: High-throughput screening (cHTS) and multi-modality imaging approach of SBL and 3D-US in a xenograft NOG mouse model of TCL were used to explore the *in vitro* and *in vivo* activity of pralatrexate and romidepsin in combination. Corresponding mass spectrometry based pharmacokinetic and immunohistochemistry based pharmacodynamic analysis of xenograft tumors were performed to better understand a mechanistic basis for the drug: drug interaction.

Results: *In vitro*, pralatrexate and romidepsin exhibited concentration-dependent synergism in combination against a panel of TCL cell lines. In a NOG murine model of TCL, the combination of pralatrexate and romidepsin exhibited enhanced efficacy compared with either drug alone across a spectrum of tumors using complimentary imaging modalities such as SBL and 3D-US.

Conclusions: Collectively, these data strongly suggest that the combination of pralatrexate and romidepsin merit clinical study in patients with TCLs.

TRANLSATIONAL RELEVANCE

Four new drugs have been approved in TCL, including 2 histone deacetylase (HDAC) inhibitors, an antibody drug conjugate (ADC) and pralatrexate. The recent approval of these agents creates the prospect that drugs with lineage specific activity can be potentially combined, creating a new platform of care. Based on single agent activity of pralatrexate and romidepsin, we systematically explored the activity of these agents in combination, employing new imaging techniques. Detailed pharmacologic analysis of drug disposition in these models, including intratumoral concentrations, reveals that pralatrexate and romidepsin are markedly synergistic *in vivo*, and that even lower doses achieve highly synergistic concentrations in plasma and tumor, resulting in marked remissions and an overall survival benefit for the combination. These observations have led to a Phase I-II clinical trial, now actively accruing. We believe this will hasten the prioritization of promising drug combinations to be studied in patients with peripheral T-cell lymphoma (PTCL).

Introduction

Peripheral T-cell lymphomas (PTCLs) represent a heterogeneous group of lymphoma's with a poor prognosis (1). Only 10-15% of patients will experience long-term survival with standard CHOP-based chemotherapy (2). While advances have been made to improve the outcome, a host of factors have contributed to poor outcomes. Intrinsic drug resistance, rapid acquisition of acquired drug resistance, and the use of regimens extrapolated from B-cell lymphomas are among the most commonly cited explanations for the observed differences in outcome between B- and T-cell lymphomas. Since 2009, four new drugs have been approved for patients with relapsed or refractory PTCL, including pralatrexate, romidepsin and belinostat for PTCL, and brentuximab vedotin for patients with CD30 positive anaplastic large cell lymphoma. All drugs have overall response rate (ORR) ranging from 26-41%, in roughly similar populations, all with similar durations of benefits (3-5). Interestingly, these single agents seem to produce benefits in excess of what one might expect for conventional chemotherapy, suggesting that their differing mechanisms of action may overcome acquired drug resistance. The collective experience with these drugs to date suggests these agents may have lineage-specific activity in TCL

The prospect to improve the outcomes of patients with PTCL will rely on our ability to identify agents with potentially selective activity in TCL, and to explore the potential merits of their combinations. A major challenge in the context of TCLs has been the limitation of reasonable preclinical models that can be used for validation of novel therapeutic approaches. *In vitro* studies of novel agents have been hindered by the fact that neoplastic T-cells are difficult to grow in culture and deriving cell lines from primary tumors is challenging. Moreover, in certain diseases like mycosis fungoides (MF), skin lesions contain both malignant and reactive benign T-cells, and discriminating between the two populations can be difficult (6). Mouse models that can be used for rapid non-invasive spatiotemporal tracking of tumor responses to new drugs and combinations are lacking in TCL research, and thus have hampered advances in the field (7, 8). New developments in *in vivo* imaging using dual-functioning reporters that are both fluorescent and bioluminescent (BLI) provide maximum experimental flexibility enabling unique

biological applications (9-12). More precise and reproducible techniques like three-dimensional ultrasound (3D-US) imaging and BLI are increasingly being used for volumetric analysis of xenograft tumor (13). However this remains to be validated in the context of lymphoma models.

We report on the development of a novel BLI xenograft mouse model of human TCL. We explore the activity of pralatrexate and romidepsin in this model and utilize a multi-modality imaging approach to validate the response across all treatment groups. The accurate and reproducible imaging techniques allowed us to use fewer animals to obtain statistically meaningful results. These observations were confirmed *in vitro* across TCL cell lines using cHTS. These results demonstrate that the combination of these agents is highly effective *in vitro* and *in vivo,* and has led to the initiation of a phase I-II clinical trial. Accompanying pharmacokinetic and pharmacodynamic analyses provide a robust rationale for the superior efficacy of this regimen. We believe that this approach could hasten the translation of interesting therapeutic strategies in PTCL to the clinic.

Materials and Methods

Cells line and Culture Condition. H9, HH and HuT-78 TCL cell lines were obtained from ATCC (Manassas, VA) (14). All cell lines were grown as previously described (15-17). All cell lines were authenticated from a hematopathologist including verification of morphology and immunophenotype.

Combination High-Throughput Screening (cHTS) Procedure. H9 and HH cell lines were plated at optimal density into 384 well tissue culture plates (Greiner 781080) at 50µL per well, incubated for 24 hours before drug addition (18). A total of 10 concentrations per drug in the combination were added in three plate replicates with DMSO (0.2%). Drugs were added using HP D300 Digital Dispenser. Twenty-five µL of Cell Titer Glo (Promega) was added and viability measured at 24, 48 and 72 hours. The standard reference model of Bliss independence was employed. Bliss predicts the combined response C for two single compounds with effects A and B is $C= A + B – A \times B$, where each effect is expressed as fractional inhibition between 0 and 1[19]. The difference between Bliss expectation and observed growth

inhibition induced by the combination of agent A and B at the same dose is the “Bliss excess” (18, 19).

RNA Analyses.

Total RNA was isolated with Trizol reagent (Invitrogen). RNA (1µg) was reverse transcribed using a commercially available cDNA synthesis kit (Bioline). Quantitative PCR was performed on RNA that was reverse transcribed with random primers (Invitrogen) and amplified in a LightCyclerThermocycler using probes from the Roche Universal ProbeLibrary (Roche Diagnostics). Primers and probe sets are shown in Supplementary Table 1. Each experiment was repeated 3–4 times. Induction of each mRNA was expressed relative to the untreated control, after normalization to rRNA.

Transfection of Cell Lines. The H9 and HuT-78 cell lines were transfected with the previously described pGLCherryluciferase plasmid using the transfection reagent, Effectene (12).

Analysis and Sorting of Transfected Cells by Flow Cytometry. Cells were harvested 48 hours post-transfection, washed and re-suspended in PBS. The cells were analyzed for mCherry expression and sorted using the MoFlo Legacy cell sorter (Beckman Coulter, Brea, CA). The sorted cells were propagated and followed by repeated sorting until a stably transfected cell line wherein >80% H9 and HuT-78 cells demonstrating fluorescent activity *in vitro* was achieved.

Mouse Xenograft Models and In Vivo Bioluminescence Imaging. *In vivo* experiments were performed as follows: 5- to 7- week old female NOD/Shi-scid/IL-2Rγ^{null} (NOG) mice (Taconic Farms, Germantown, NY) were injected with up to 2 million mCherryluciferase expressing H9 cells in subcutaneously in the. *In vivo* BLI analysis was conducted on a cryogenically cooled IVIS system (Xenogen Corp, California,USA) as previously described (12). Initial experiments explored complementary anti-tumor effects and toxicities of various doses and schedules of romidepsin and pralatrexate in these mice. Drugs were administered by intraperitoneal (i.p) injection as follows: romidepsin 1.2mg/kg and 2mg/kg on days 1, 4, 8 and 11 and 3mg/kg weekly for 3 of 4 weeks; and pralatrexate 15mg/kg and 30mg/kg on days 1, 4, 8 and 11. Based on these results, a subsequent experiment was performed, where mice were inoculated in the flank with 2 million H9-mCherryluciferase cells. Animals were randomized into 4 groups of 6 animals each as follows:

(1) control group treated with normal saline alone; (2) romidepsin group in which the drug was administered at 2mg/kg on days 1, 8 and 14; (3) pralatrexate group in which the drug was administered at 15mg/kg on days 1, 4, 8 and 11 and (4) combination group of romidepsin and pralatrexate at the same dose and schedule as single agent groups. Assignments were made by order of intensity to the treatment groups to assure that the average starting signals within all groups were similar. Baseline BLI was recorded for all mice on day 1 (start of drug administration) and on each day of drug administration before the treatment. Romidepsin and pralatrexate were administered by i.p injection. All the mice were monitored twice a week and sacrificed if they become ill, were unable to eat or drink, or if the tumor hindered normal body movement as promulgated by IACUC regulations. A similar xenograft tumor experiment with equivalent doses and schedules of romidepsin and pralatrexate was performed with the mCherryluciferase expressing HuT-78 cells.

Mouse Xenograft Model and Ultrasound Imaging. In a second parallel *in vivo* experiment, 5- to 7-week-old female NOG mice were injected with 2 million H9 cells subcutaneously in the flank. Three-dimensional ultrasound imaging data sets were collected for each xenograft using a Vevo2100 ultrasound microimaging system (VisualSonics Inc, Ontario, Canada) designed for small animal imaging. For imaging acquisition, mice were anesthetized using 2% isofluorane in oxygen followed by placement on a heated stage during the course of imaging. Anesthesia was maintained during imaging using 2% isoflurane in oxygen. Xenografts were coated with warmed (37°C) Aquasonic 100 ultrasound gel (Parker Laboratories, New Jersey, USA) and centered in the imaging plane. Three-dimensional B-mode data was acquired by automated translation of the 30MHz ultrasound transducer along the entire length of the xenograft. The resulting data sets had a 17mm×17mm field of view with an in-plane pixel resolution of 33.2×33.2μm and an interslice spacing of 101.6μm, resulting in 33.2×33.2×101.6μm voxels. For analysis of ultrasound data, images were imported into Amira 5.2 (Visage Imaging, San Diego, California) for volumetric analysis. Tumor tissue was hypoechoic relative to non-tumor tissue. Tumor volume was determined by summation of the in-plane segmented regions and multiplying this quantity by the inter-slice spacing as described (13). Mice were imaged twice a week starting 4 days after inoculation of cells. Once xenograft tumors

reached an average of 3-5mm on imaging, mice were randomized to 4 treatment groups of 9 animals each: (1) control group treated with normal saline alone; (2) romidepsin group that received 2mg/kg of drug on days 1, 8 and 14; (3) pralatrexate group that received 15mg/kg of drug on days 1, 4, 8 and 11 and (4) combination group of romidepsin and pralatrexate at the same dose and schedule as single agent groups. Baseline imaging data was recorded for all mice on day 1 (start of drug administration) and on each day of drug administration before the treatment. All the mice are monitored twice a week and managed as per IACUC regulations.

Quantification of Romidepsin and Pralatrexate in Mouse Plasma and Tumor tissue. To define and compare the pharmacokinetic profile of the two agents and their combination in blood and tumor tissue, serial blood collections were performed at 6, 18 and 24-hours after the first dose administration in three mice from each group in the BLI experiment. After the 24-hour blood collection, mice were euthanized and tumor tissue was harvested. Plasma was prepared by centrifugation at room temperature. Plasma and tumor tissue were stored at -80ºC prior to analysis. Romidepsin and pralatrexate were quantified using 25µl of plasma or ~ 20mg of tumor tissue. Tissue was homogenized in 100µl of saline using a 1ml dounce homogenizer. The homogenate was rinsed with 100µl of saline. Proteins from plasma and tumor homogenates were precipitated with 1ml of acetonitrile/methanol (4:1). After vortexing for 60seconds the samples were centrifuged (14000xG for 10min). Supernatant was evaporated with nitrogen and resolubilized with 75ul of 10% methanol. Five µl of each sample was injected onto a Poroshell 120 EC-C18 2.1x50mm 2.7-micron column (40˚C; Agilent Technologies, USA) using an Agilent 1290 Infinity UHPLC (Agilent Technologies) with the initial conditions 100% 0.1% formic acid in water (0.5ml/min) and ramped linearly to 40% 0.1% formic in acetonitirile over 3minutes. The column was cleaned with 95% of 0.1% formic acid in acetonitirile for 1minute and then re-equilibrated to the initial conditions for 1.8minutes (total run time: 6.3minutes). Romidepsin and pralatrexate were detected with an Agilent6410 tandem mass spectrometer with positive electrospray ionization. Drugs were quantified using multiple reactions monitoring of the +H ion with the transition 541.2 to 424.1 (collision energy= 13V; Fragmentor=135V) and

478.2 to 175.1 (collision energy= 29V; Fragmentor=175V) for romidepsin and pralatrexate respectively. Spiked plasma was used to create a standard curve, which was linear from 1ng/ml to 2500ng/ml with a LOQ and LOD of 1.0ng/mL and 0.5ng/mL respectively. Quantification of romidepsin and pralatrexate in both plasma and tumor tissue was calculated relative to the spiked plasma standard curve. The MS conditions were as follows: gas temperature=300 C; Gas Flow=13l/min; nebulizer=45psi; capillary=4500v; desolvation gas flow=500 L/hr; cone gas flow=50 L/hr; collision energy=30 V.

Morphology and Immunohistochemistry for Cell Proliferation and Apoptosis. Twenty-one days after drug administration in the BLI intensity H9 xenograft experiment, mice were euthanized, tumors were excised and weighed. One part was fixed in 10% neutral-buffered formalin overnight before processing, embedded in paraffin and sections (4 μm) were stained with Hematoxylin and Eosin to determine presence of tumor for immunohistochemistry. The remainder was stored at -80ºC. One 5 μm section of tissue was examined by hematoxylin–eosin staining to verify that adequate tumor tissue was present, blocks were then randomly arrayed in a 4mm tissue array (three tumors per group in and two sections per marker). Immunohistochemical staining was performed after 5μm sections from these arrays were used. After deparaffinization of tissue sections, endogenous peroxidase was blocked by 3% H_2O_2, and endogenous avidin and biotin was blocked according to the supplied protocol (Vector, California, USA). Bromodeoxyuridine (BrdU) labeling of tumor cell nuclei was performed by I.P. injection, 0.2mL of BrdU solution (Cell Proliferation Labeling Reagent; GE Healthcare Life Sciences, Piscataway, NJ) 2-hours before harvesting. Mice were sacrificed, tumors excised, and tumor-incorporated BrdU was stained with the BrdU In-Situ Detection Kit (BD Pharmingen, San Diego, CA), according to the supplied protocol. The formalin-fixed and paraffin-embedded 5μm thick sections of all tumor samples were used to identify apoptotic cells by terminal uridine deoxynucleotidyl transferase dUTP nick end labeling (TUNEL) staining using tumor TACS in situ apoptosis detection kit (R & D Systems, Inc) as detailed recently (20). Tumors were scored by the percentage of cells positive for BrdU (as a measure of cell proliferation), necrosis and

for TUNEL (as a measure of apoptosis) using an Olympus BX41microscope, total magnification×400 (Olympus America Inc., New York).

Statistical Analysis. Log-linear mixed models were used to model the tumor intensity in the BLI experiment groups or 3D tumor volume in the US group (21). The model assumed that the logarithm of the tumor intensity (or volume) is linear in time, and allowed difference intercepts and slopes for different treatment groups. A random effect of individual mice to account for the within-mouse correlation was also included in the model. The expected tumor intensities (or volumes) on the 4^{th}, 8^{th}, 11^{th}, 14^{th}, and 18^{th} day were estimated from the model. Due to the small sample sizes, permutation tests were performed to determine whether the single-drug experimental groups and the control group were significantly different from the combination group on each of the days. The Kaplan-Meier survival functions were calculated respectively for each group. Log-rank test was used to compare the median survival times among the treatment groups.

Results.

Romidepsin and Pralatrexate is Synergistic in T-cell Lymphoma Lines. A high throughput screening protocol (cHTS) and Bliss Independence was used to quantitate synergy (18, 19). Two cell lines, H9 and HH were treated with romidepsin at the IC_{10} or IC_{20} (corresponding to 2nM either alone or in combination with pralatrexate at concentrations ranging from 20nM to 1μM (IC_{10}-IC_{60}), and evaluated following 24, 48 and 72-hours of exposure. Excess over Bliss (EOB) scores are presented (Tables A and B, Figure 1). Synergy was observed over a range of concentrations in both cell lines. EOB scores of >10 represent synergy. Full matrix of the (cHTS) results highlighting synergy in H9 and HH cell lines at 48 and 72 hours respectively are included in Supplementary Figure 1. There was no observed difference of the combination at 24 hours compared to any of the single drug treatments

RNA Analyses of Folate Pathway Gene Expression

A potential synergistic mechanism would be to increase levels of RFC (Reduced folate carrier) or FPGS (Folylpolyglutamate synthase), which would promote intracellular retention of pralatrexate. We examined gene expression following the combination of romidepsin and pralatrexate, and the drugs alone at 12, 24, and 48-hours. Additionally, romidepsin has been shown to induce expression of drug resistance genes including ABCG2 (ATP-binding cassette, sub-family G, member 2), a potential mechanism of resistance for pralatrexate (22-24). While positive controls for romidepsin gene induction were confirmed, no alterations were observed in combination with pralatrexate in the RFC, DHFR (Dihydrofolate reductase), GGH (Gamma-glutamyl hydrolase), FPGS, or ABCG2 genes in any of the 3 cell lines (Figure 1C, 24-hour data). While RNA induction did not explain the synergistic effects with the HDAC inhibitor, it also would not interfere with cell death induced independently by the two agents.

Development of a Bioluminescent Xenograft Mouse Model of Human T-Cell Lymphoma. Stable cell lines of H9 and HuT-78 expressing mCherry and luciferase were generated (Supplementary Figure 2). Various routes (subcutaneous, intravenous) and concentrations (up to 20 million cells) of H9mCherryluciferase cells were injected into 5- to 7-week-old SCID/Beige mice. No evidence of tumor engraftment was noted. We then investigated the engraftment of the mCherryluciferase expressing H9 and HuT-78 cells in NOD/Shi-scid/IL-2R^{null} (NOG) mice. Two million cells were injected subcutaneously in the flank of 5- to 7-week-old female NOG mice. Bioluminescent imaging was initiated 48-hours after inoculation of cells and demonstrated uniform linear increase in light intensity over time at the site of tumor cell injection suggesting engraftment in all mice. Exploratory toxicity experiments were performed (Figure 2). When 1.2 mg/kg of romidepsin was administered on days 1, 4, 8 and 11, there was minimal effect on tumor intensity (Figure 2A). Administration of 30 mg/kg of pralatrexate on days 1, 4, 8 and 11 produced rapid and complete tumor reduction, though more than 50% of animals experienced hemorrhagic ascites likely secondary to thrombocytopenia (Figure 2B). When 2mg/kg of romidepsin was administered on days 1, 4, 8 and 11, there was modest growth delay, but >50% of the mice experienced

>10% weight loss suggestive of toxicity (Figure 2C). Administration of 15 mg/kg of pralatrexate on days 1, 4, 8 and 11 induced minimal tumor regression but was well tolerated (Figure 2D). Four of five mice administered 3mg/kg of romidepsin weekly died within 1-week of administration of the first dose due to sudden deaths with no obvious cause evident on necropsy. Based on these data, mice inoculated with mCherryluciferase expressing H9 cells were randomized to one of four groups of treatment (n=6 in each cohort): (1) a control group treated with normal saline alone; (2) a romidepsin group administered 2mg/kg on days 1, 8 and 14; (3) a pralatrexate group administered 15mg/kg on days 1, 4, 8 and 11 and (4) a combination group of both drugs administered at the same dose and schedule as above. After 21 days from the start of treatment, the combination group treated demonstrated a statistically significant reduction in the bioluminescent intensity compared to the romidepsin alone ($p<0.05$), pralatrexate alone ($p<0.05$), and control ($p<0.05$) groups (Figure 3A and B). Complete remissions (CRs) were observed by day 18 only in the combination cohort where all 6 mice experienced CR. Neither significant weight loss nor death was observed in any of the cohorts (Day 21) when all mice were euthanized to harvest tumor.

Pharmacodynamic Analysis of Romidepsin and Pralatrexate in Xenograft Tumors by Immunohistochemistry. Given the statistically significant tumor growth inhibition by the combination treatment (Figure 3), we analyzed its effect on necrosis and apoptosis by TUNEL staining. Quantification of necrosis and TUNEL-positive apoptotic cells were increased in the combination mouse (80% and 75%, respectively) compared to control (40% and 15% respectively), romidepsin alone (60% and 25% respectively) and pralatrexate alone (60% and 38%, respectively) shown in Figure 3C and 3D. We investigated cell proliferation by assessing the uptake of BrdU by tumor cells. A representative histogram of BrdU staining from a mouse xenograft tumor from each treatment group is depicted in Figure 3D. The fraction of actively proliferating cells was lower in the combination mouse (20%) compared to control (60%), romidepsin alone (40%) and pralatrexate alone (40%) treated mice in agreement with the gross decrease in tumor burden noted in the combination group compared with control and other treatment groups. These effects were confirmed in the HuT-78 xenograft tumors (Figure 4). These data validate the utility of the BLI xenograft murine model of humanTCL, and supports our original hypothesis.

Therapeutic Effects of in High Volume Tumors by Three-Dimensional Ultrasound. The *in vivo* efficacy of the combination observed in the BLI experiment was investigated in another xenograft experiment, using higher tumor starting volumes using 3D-US. Two-million mCherryluciferase expressing H9 cells were injected subcutaneously in the flank of 5- to 7-week-old female NOG mice. Three-dimensional ultrasound imaging data sets were collected for each xenograft starting 4 days after inoculation of tumor cells twice a week. Once the diameter of the xenograft tumors reached 3-5 mm corresponding to 70-90mm^3 tumor volume on US imaging, mice were randomized to one of the 4 treatment groups (n=9 in each cohort) including: (1) a control group treated with normal saline alone; (2) a romidepsin group administered 2mg/kg on days 1, 8 and 14; (3) a pralatrexate group in which administered 15mg/kg on days 1, 4, 8 and 11 and the (4) combination group received drugs at the same dose and schedule as the single agent groups. The average tumor volume at the start of treatment was similar under standardized imaging conditions. Twenty-one days from the start of treatment the mice administered the combination demonstrated a statistically significant reduction in their 3D tumor-volumes compared to romidepsin alone ($p<0.05$), pralatrexate alone ($p<0.05$) and control ($p<0.05$) groups (Figure 5A and B). Further, 8 of 9 mice treated in the combination cohort experienced complete remissions (CRs) by day 21, with 3 of those complete remissions being maintained beyond day 30. Neither significant weight loss nor death was observed in any of the cohorts.

Survival analysis of mice in the ultrasound group. Treatment was terminated after 1 cycle of therapy (3 weeks) across all treatment groups. Mice were subsequently followed for survival analysis until they had to be euthanized for disease progression. Kaplan-Meier survival functions were calculated for each group and demonstrated that survival distributions for the 4-treatment groups were significantly different in general (Figure 5C). Log-rank test for comparison of median survival time among the four treatment groups (control, romidepsin alone, pralatrexate alone and romidepsin plus pralatrexate) exhibited marked increase in survival for the combination group versus all other cohorts (Figure 5D).

Preclinical pharmacokinetic analysis of romidepsin and pralatrexate in mouse plasma and tissues by high affinity liquid chromatography and tandem mass spectrometry (HPLC-MS/MS). A HPLC-MS/MS method was developed for the simultaneous quantification of romidepsin and pralatrexate, in mice plasma and tissues. The method is selective and highly sensitive with a detection limit of 0.5ng/mL in plasma. The concentration of romidepsin and pralatrexate in mice plasma samples at 6, 18 and 24 hours after the first I.P. dose administration in 3 mice from each group in the BLI H9 xenograft experiment were determined by this method. Intratumoral drug concentrations were quantified by this method 24-hours after the first dose. The mean plasma concentration of romidepsin versus time curves and pralatrexate versus time curves is presented in Figures 6A and 6B respectively. Relatively high concentrations were achieved at 6-hours after intra-peritoneal injection for both drugs. Plasma levels then declined and were undetectable in most samples by 24 hours. Mean concentrations of romidepsin and pralatrexate in tissue 24 hours after injection are depicted in Figures 6C and 6D respectively with no statistically significant differences in intra-tumoral concentrations. These data demonstrate an unchanged pharmacokinetic profile of romidepsin in mouse plasma and tissue despite the presence of pralatrexate. Despite low levels of the two agents in plasma at 24 hours, both drugs were retained at high concentrations in the xenograft tumor tissue, which may potentially explain the efficacy of the combination.

Discussion

The TCLs represent a heterogeneous group of diseases with few to no preclinical tools to assess drug activity. Given the rapidly emerging number of drugs in these malignancies, coupled with their relative rarity, it is imperative we develop models that allow us to establish pharmacologic principles that hasten the translation of new treatment strategies for PTCL. Laboratory studies of PTCL typically relied on a limited range of cell lines including anaplastic large cell lymphoma, acute T-cell leukemia, and transformed MF, which may or may not be representative of the broader disease entity. There are no well-established cell lines representing subtypes like angioimmunoblastic TCL, PTCL-NOS, and others.

Short term culturing of primary TCL derived cells such as Sezary cells is possible but establishment of long-term cultures of cells has proven to be exceedingly difficult. Further it can be questioned whether *in vitro* studies using these lines are representative of the *in vivo* circumstance, as few well-described *in vivo* models of TCL exist (25, 26). One objective of these studies was to develop a non-invasive *in vivo* model and generate a 'proof-of-concept' study demonstrating both efficacy of the combination *in vivo*, and to define pharmacologic features. We began with pralatrexate and romidepsin as these were the first drugs approved for relapsed/refractory PTCL.

Most of the available published models have not been employed for evaluating experimental drugs and their combinations, or for determining their pharmacokinetic and pharmacodynamic profile for translation to early phase clinical trials. Few of the current *in vivo* models use non-invasive imaging techniques and are not optimized to measure tumor specific variables or plasma: tumor drug ratios. Romidepsin and pralatrexate are the first two agents approved for the treatment of relapsed/refractory PTCL. These agents, in addition to a host of others now emerging, raise the prospect that new small molecules with lineage specific activity could be combined to develop novel treatment platforms for TCL. Making an assumption that every doublet - when configured strictly on the basis of single agent activity in a clinical context - will be complementary in combination is flawed. To prioritize the potential clinical study of these combinations, we need better preclinical tools to better explore the merits of novel combinations.

Initial *in vitro* studies based on cHTS and a Bliss independence model demonstrated synergy of romidepsin and pralatrexate across TCL lines. Initial attempts to engraft the H9 TCL cell line in SCID/Beige mice, were unsuccessful. Subsequently, NOG mice permitted 100% engraftment of both H9 and HuT-78 suggesting that it may be a superior xenotransplantation recipient. This strain of mouse is being increasingly used as a xenotransplantation tool in a variety of hematologic and solid tumor malignancies (27, 28). One of the limitations of this murine model is the inability to assess the influence of the tumor microenvironment on tumor progression and growth due to the immunological deficits of the

mice. Another drawback may include the inability to examine the influence of specific genes in tumor progression and response to therapy. Subsequent experiments concentrating on identifying the dose and schedule of romidepsin and pralatrexate for combination studies demonstrated that the maximum tolerated dose (MTD) of these agents varied with the strain of mice being used. Previous work from our laboratory demonstrated that in SCID/Beige mice the MTD of pralatrexate was 60mg/kg on days 1, 4, 8 and 11 where as in this NOG mouse model even the 30mg/kg dose twice weekly proved toxic albeit effective (16). At the doses used for combination studies neither of the drugs exhibited significant anti-tumor activity as single agents. However, when they were used in combination a statistically significant marked reduction in tumor burden leading to increased survival was observed. These findings underscore the synergistic activity of the combination regimen *in vivo*. The intensity of the BLI signal in murine models using luciferase transfected cells can be reliably used as a surrogate for tumor volume in tracking growth and regression in response to drugs and their combinations[12]. One criticism of these strategies is that these models may recapitulate disease states with a very low tumor burden, which might select for better therapeutic activity than actually exists under clinical scenarios. In order to address this consideration, we adopted a strategy in which we investigated xenograft tumor responses across a greater spectrum of volumes in a parallel experiment with an additional imaging modality like 3D-US. We observed that despite the differences in techniques and the tumor burden at the start of treatment, the results were strikingly similar. Even in these more challenging treatment scenarios, the romidepsin and pralatrexate combination emerged as superior in effecting tumor reduction compared with control and single agents. Our data suggest that surface BLI imaging may be useful in tracking early tumor engraftment and response in drug intervention studies. A complimentary imaging modality like ultrasound may be more beneficial in monitoring tumor burden in advanced stages of disease. Hence, the integration of these two monitoring approaches could provide a more comprehensive evaluation of tumor response in *in vivo* models.

Clear explanations for the effectiveness of good combinations in clinical oncology are often elusive. In the case of romidepsin and pralatrexate, several possibilities exist. Pralatrexate preferentially enters cancer cells via the RFC, has increased intracellular retention due to polyglutamylation, and impairs DNA synthesis via inhibition of DHFR (29). We investigated whether romidepsin would increase the levels of proteins that promote intracellular retention (or conversely, reduce the levels), but saw no impact at the RNA level. However, HDAC inhibitors including romidepsin have been shown to induce DNA damage through both acetylation-mediated events and inhibition of DNA repair. Thus, romidepsin might block recovery of DNA synthesis following its inhibition by pralatrexate. Confirmation of the combination activity in the clinic will provide the impetus to understanding the mechanism in detail. Pharmacokinetic and pharmacodynamic studies were performed on both the individual mouse, tumor, and tumor cells. HPLC-MS/MS based quantification of drug concentrations in mouse plasma and tumor tissue highlighted that the kinetics of the two agents were not antagonistic and did not adversely affect the activity of the other drug. Both agents were retained in the tumor tissue at higher levels even when their corresponding plasma levels were undetectable, which provides a robust rationale for the rapid activity seen by this combination, and the selective accumulation of these drugs in the target tumor. Immunohistochemical studies of xenograft tumor tissue confirmed a greater inhibition of cell proliferation and apoptosis with the combination in comparison with single agents and control groups.

In summary, we have developed a BLI mouse model of human TCL to rapidly screen promising agents and their combinations in a non-invasive longitudinal fashion. Our preclinical murine data demonstrate that the combination of romidepsin and pralatrexate was an effective strategy in tumor reduction in comparison to the single agents. The multi-modality approach we adopted to evaluate this strategy was able to screen for the activity of this regimen against a wide spectrum of tumor volumes and may offer researchers greater confidence in preclinical drug development. These results were supported by the correlative pharamacokinetic and pharmacodynamic data. An early phase I/IIA clinical trial to investigate this combination started.

ACKNOWLEDGEMENTS

We are grateful to the Columbia University Lymphoma Research Fund for support. Imaging studies were performed in collaboration with the Small Animal Imaging Shared Resource within the Herbert Irving Comprehensive Cancer Center (NCI 3 P30 CA13696). The Vexo 2100 ultrasound was purchases from a Small Instrumentation Grant (S 10 RR025482-01AS10).

References

1. Vose J, Armitage J, Weisenburger D, International TCLP. International peripheral T-cell and natural killer/T-cell lymphoma study: pathology findings and clinical outcomes. J Clin Oncol. 2008;26(25):4124-30.
2. Simon A, Peoch M, Casassus P, Deconinck E, Colombat P, Desablens B, et al. Upfront VIP-reinforced-ABVD (VIP-rABVD) is not superior to CHOP/21 in newly diagnosed peripheral T cell lymphoma. Results of the randomized phase III trial GOELAMS-LTP95. Br J Haematol. 2010;151(2):159-66.
3. O'Connor OA, Pro B, Pinter-Brown L, Bartlett N, Popplewell L, Coiffier B, et al. Pralatrexate in patients with relapsed or refractory peripheral T-cell lymphoma: results from the pivotal PROPEL study. J Clin Oncol. 2011;29(9):1182-9.
4. Coiffier B, Pro B, Prince HM, Foss F, Sokol L, Greenwood M, et al. Results from a pivotal, open-label, phase II study of romidepsin in relapsed or refractory peripheral T-cell lymphoma after prior systemic therapy. J Clin Oncol. 2012;30(6):631-6.
5. Horwitz SM, Advani RH, Bartlett NL, Jacobsen ED, Sharman JP, O'Connor OA, et al. Objective responses in relapsed T-cell lymphomas with single-agent brentuximab vedotin. Blood. 2014;123(20):3095-100.
6. Fivenson DP, Hanson CA, Nickoloff BJ. Localization of clonal T cells to the epidermis in cutaneous T-cell lymphoma. J Am Acad Dermatol. 1994;31(5 Pt 1):717-23.
7. van der Fits L, Rebel HG, Out-Luiting JJ, Pouw SM, Smit F, Vermeer KG, et al. A novel mouse model for Sezary syndrome using xenotransplantation of Sezary cells into immunodeficient RAG2(-/-) gammac(-/-) mice. Exp Dermatol. 2012;21(9):706-9.
8. Doebbeling U. A mouse model for the Sezary syndrome. J Exp Clin Cancer Res. 2010;29:11.
9. Edinger M, Cao YA, Verneris MR, Bachmann MH, Contag CH, Negrin RS. Revealing lymphoma growth and the efficacy of immune cell therapies using in vivo bioluminescence imaging. Blood. 2003;101(2):640-8.
10. Rehemtulla A, Stegman LD, Cardozo SJ, Gupta S, Hall DE, Contag CH, et al. Rapid and quantitative assessment of cancer treatment response using in vivo bioluminescence imaging. Neoplasia. 2000;2(6):491-5.

11. Vooijs M, Jonkers J, Lyons S, Berns A**.** Noninvasive imaging of spontaneous retinoblastoma pathway-dependent tumors in mice. Cancer Res. 2002;62(6):1862-7.
12. Scotto L, Kruithof-de Julio M, Paoluzzi L, Kalac M, Marchi E, Buitrago JB, et al. Development and characterization of a novel CD19CherryLuciferase (CD19CL) transgenic mouse for the preclinical study of B-cell lymphomas. Clin Cancer Res. 2012;18(14):3803-11.
13. Graham KC, Wirtzfeld LA, MacKenzie LT, Postenka CO, Groom AC, MacDonald IC, et al. Three-dimensional high-frequency ultrasound imaging for longitudinal evaluation of liver metastases in preclinical models. Cancer Res. 2005;65(12):5231-7.
14. Gootenberg JE, Ruscetti FW, Mier JW, Gazdar A, Gallo RC**.** Human cutaneous T cell lymphoma and leukemia cell lines produce and respond to T cell growth factor. J Exp Med. 1981;154(5):1403-18.
15. Toner LE, Vrhovac R, Smith EA, Gardner J, Heaney M, Gonen M, et al. The schedule-dependent effects of the novel antifolate pralatrexate and gemcitabine are superior to methotrexate and cytarabine in models of human non-Hodgkin's lymphoma. Clin Cancer Res. 2006;12(3 Pt 1):924-32.
16. Marchi E, Paoluzzi L, Scotto L, Seshan VE, Zain JM, Zinzani PL, et al. Pralatrexate is synergistic with the proteasome inhibitor bortezomib in in vitro and in vivo models of T-cell lymphoid malignancies. Clin Cancer Res. 2010;16(14):3648-58.
17. O'Connor OA, Smith EA, Toner LE, Teruya-Feldstein J, Frankel S, Rolfe M, et al. The combination of the proteasome inhibitor bortezomib and the bcl-2 antisense molecule oblimersen sensitizes human B-cell lymphomas to cyclophosphamide. Clin Cancer Res. 2006;12(9):2902-11.
18. Borisy AA, Elliott PJ, Hurst NW, Lee MS, Lehar J, Price ER, et al. Systematic discovery of multicomponent therapeutics. Proc Natl Acad Sci U S A. 2003;100(13):7977-82.
19. Berenbaum MC**.** Criteria for analyzing interactions between biologically active agents. Adv Cancer Res. 1981;35:269-335.
20. Singh RP, Mallikarjuna GU, Sharma G, Dhanalakshmi S, Tyagi AK, Chan DC, et al. Oral silibinin inhibits lung tumor growth in athymic nude mice and forms a novel chemocombination with doxorubicin targeting nuclear factor kappaB-mediated inducible chemoresistance. Clin Cancer Res. 2004;10(24):8641-7.
21. Lindstrom ML, Bates DM**.** Nonlinear mixed effects models for repeated measures data. Biometrics. 1990;46(3):673-87.
22. To KK, Polgar O, Huff LM, Morisaki K, Bates SE**.** Histone modifications at the ABCG2 promoter following treatment with histone deacetylase inhibitor mirror those in multidrug-resistant cells. Mol Cancer Res. 2008;6(1):151-64.
23. To KK, Robey R, Zhan Z, Bangiolo L, Bates SE**.** Upregulation of ABCG2 by romidepsin via the aryl hydrocarbon receptor pathway. Mol Cancer Res. 2011;9(4):516-27.
24. Breedveld P, Pluim D, Cipriani G, Dahlhaus F, van Eijndhoven MA, de Wolf CJ, et al. The effect of low pH on breast cancer resistance protein (ABCG2)-mediated

transport of methotrexate, 7-hydroxymethotrexate, methotrexate diglutamate, folic acid, mitoxantrone, topotecan, and resveratrol in in vitro drug transport models. Mol Pharmacol. 2007;71(1):240-9.

25. Chiarle R, Gong JZ, Guasparri I, Pesci A, Cai J, Liu J, et al. NPM-ALK transgenic mice spontaneously develop T-cell lymphomas and plasma cell tumors. Blood. 2003;101(5):1919-27.
26. Pechloff K, Holch J, Ferch U, Schweneker M, Brunner K, Kremer M, et al. The fusion kinase ITK-SYK mimics a T cell receptor signal and drives oncogenesis in conditional mouse models of peripheral T cell lymphoma. J Exp Med. 2010;207(5):1031-44.
27. Imadome K, Yajima M, Arai A, Nakazawa A, Kawano F, Ichikawa S, et al. Novel mouse xenograft models reveal a critical role of CD4+ T cells in the proliferation of EBV-infected T and NK cells. PLoS Pathog. 2011;7(10):e1002326.
28. Patel S, Zhang Y, Cassinat B, Zassadowski F, Ferre N, Cuccuini W, et al. Successful xenografts of AML3 samples in immunodeficient NOD/shi-SCID IL2Rgamma(-)/(-) mice. Leukemia. 2012;26(11):2432-5.
29. Izbicka E, Diaz A, Streeper R, Wick M, Campos D, Steffen R, et al. Distinct mechanistic activity profile of pralatrexate in comparison to other antifolates in in vitro and in vivo models of human cancers. Cancer Chemother Pharmacol. 2009;64(5):993-9.

Figure Legends

Figure 1 (Table A and B). *In vitro* synergy of romidepsin and pralatrexate in T-ell lymphoma cell lines. High throughput screening procedure was used to explore the combination of romidepsin and pralatrexate in vitro in TCL cell lines H9 and HH. Romidepsin was dosed at 0.002 μM and pralatrexate was dosed in a range of 0.02 to 1 μM after testing 10 different concentrations of each drug. Based on the excess over bliss model, values >10 were suggestive of synergistic effect of combination versus additive. Each value reported is the average of at least 3 independent experiments run in triplicate. H9 cell line demonstrated synergy at 48 hours where as HH exhibited synergistic effect at 72 hours as exhibited in Tables A and B respectively. *There was no observed difference of the combination at 24 hours compared to any of the single drug treatments.

Figure 1(C). Heat map showing quantitative PCR analysis of RNA expression following romidepsin and pralatrexate. Response of genes with potential impact on pralatrexate (PDX) sensitivity or resistance are shown. Positive controls, B1 [ABCB1 (ATP-binding cassette, sub-family G, member 1) or MDR1 (Multi-drug resistance gene)], FOS (Proto-oncogene c-FOS), and p21, often found upregulated in response to romidepsin (Romi) are shown for each cell line. Genes with potential impact on pralatrexate intracellular retention or resistance: ABCG2 (ATP-binding cassette, sub-family G, member 2); gamma-glutamyl hydrolase (GGH); folylpolyglutamate synthase (FPG), dihydrofolate reductase (DHFR); and reduced folate carrier (RFC). Scale is shown next to the figure ranging from X to X-fold induction.

Figure 2. Determination of maximum tolerated dose for romidepsin and pralatrexate and associated anti-tumor activity. *In vivo* surface bioluminescence acquired images of H9 human T-cell lymphoma xenograft tumors in mice with corresponding mean BLI response to intraperitoneal (i.p) treatment with: romidepsin 1.2 mg/kg dose, showed minimal effect on tumor reduction but was well tolerated (A), pralatrexate 30 mg/kg dose, demonstrated marked anti-tumor activity but associated with high toxicity (B), romidepsin 2 mg/kg dose, exhibited modest activity but associated with toxicity (C), pralatrexate 15 mg/kg dose, revealed minimal anti-tumor activity but was well tolerated (D). All drugs were administered on days 1, 4, 8 and 11.

Figure 3. Analysis of bioluminescent intensity (BLI) of H9 xenograft tumors to romidepsin and pralatrexate. *In vivo* surface bioluminescence images were acquired (n=6 in each group) to determine tumor response of H9 xenograft to intraperitoneal (i.p.) treatment with romidepsin and pralatrexate. A

control group was administered normal saline on days 1, 4, 8, 11, 14. Two single agent cohorts received treatment with romidepsin 2 mg/kg dose on days 1, 8 and 14, and pralatrexate 15 mg/kg dose on days 1, 4, 8 and 11. A combination cohort received simultaneous treatment with romidepsin and pralatrexate at the same dose and schedule as single agent groups. All cohorts were imaged on days 1, 4, 8, 11, 14, 18 and 21 using IVIS Spectrum Imaging System before administration of drugs. Tumor location is highlighted by BLI (A). After acquisition of images a mean BLI curve of human H9 xenografts was generated. The combination arm demonstrated a greater decline in their BLI from day 4 after the start of treatment in comparison with the other cohorts (B). P-value was calculated to determine the result were statistically significant at several time points in comparison to the other treatment groups. Xenograft tumor harvested from mice (n=3 in each group) 7 days after completion of one cycle of treatment (control, romidepsin, pralatrexate and romidepsin plus pralatrexate combination,) was analyzed for necrosis, apoptosis and cell proliferation. Apoptotic cells were identified by TUNEL staining. Corresponding photomicrographs of apoptosis and necrosis at different magnifications across the treatment groups are displayed in C and histogram demonstrating greater apoptosis in the combination group in contrast to the other treatment groups is displayed in D. Cell proliferation was measured through BrdU staining. The level of proliferation inhibited with romidepsin plus pralatrexate combination was higher in contrast to the other treatment groups (D).

Figure 4. *In vivo* surface bioluminescence analysis of HUT-78 human T-cell lymphoma xenograft tumors in mice and their response pralatrexate and romidepsin. *In vivo* surface bioluminescence images (BLI) were acquired (n=5 in each group) to determine tumor response of HUT-78 xenografts to intraperitoneal (i.p.) treatment with romidepsin and pralatrexate. On days 1, 8 and 14, mice were treated normal saline (control), and single agent romidepsin 2 mg/kg dose. Single agent pralatrexate 15 mg/kg was administred on days 1, 4, 8 and 11. Combination of romidepsin and pralatrexate was administered at the same dose and schedule as single agents. All cohorts were imaged on days 1, 4, 8, 11 and 14 using IVIS Spectrum Imaging System, and any respective drug dose was given after completing the imaging process. Tumor location is highlighted by the BLI (A). With the images collected we generated a mean BLI curve of human T-cell lymphoma xenografts. The combination arm demonstrated a greater decline in their BLI from day 4 onwards after the start of treatment in comparison with the other cohorts (B). P-value was calculated to show the result were statistically significant at several time points in comparison to the other treatment groups (C).

Figure 5. *In vivo* ultrasound images of H9 human T-cell lymphoma xenograft tumors in mice and their response to romidepsin and pralatrexate. *In vivo* Ultrasound (US) images were acquired (n=9 in each group) to determine tumor response of H9 xenografts to intraperitoneal (i.p.) treatment with romidepsin and pralatrexate. On days 1, 8 and 14 mice were treated i.p.with normal saline control (A-D), and single agent romidepsin 2 mg/kg (E-H). Single agent pralatrexate 15 mg/kg was administred on days 1, 4, 8 and 11(I-L). Combination of romidepsin and pralatrexate was administered at the same dose and schedule as single agents (M-P). All cohorts were imaged on days 1, 8, 14 and 21 VisualSonics Vevo 2100 Imaging System, and any respective drug dose was given after completing the imaging process. Tumor location is outlined with blue lines (A). The US system acquired sequential images for each tumor, resulting in a 3D representation of the tumors. The 3D images were used to calculate the estimated tumor volume, and generate a tumor response curve. As shown in the curve, the combination cohort demonstrated a greater decline in the estimated tumor volumes after day 4 of treatment in comparison with the other cohorts (B). P-value was calculated to determine the results were statistically significant at several time points in comparison to the other treatment groups. We followed the mice for survival, and generated Kaplan-Meier survival plot curve of the 4 cohorts in the experiment. Combination mice receiving romidepsin plus pralatrexate showed longer survival compared to other treatment groups (C). P-value, and 95% confidence interval analysis were performed to determine the survival curve was statistically significant in contrast to other treatment groups through (D).

Figure 6. Preclinical pharmacokinetic analysis of romidepsin and pralatrexate *in vivo.* High affinity liquid chromatography and tandem mass spectrometry (HPLC-MS/MS) based assay was used to calculate plasma concentrations of romidepsin and pralatrexate at 6, 18 and 24 hours after the first dose in various treatment cohorts of the H9 xenograft tumors in the BLI experiment (n=3 in each group). High levels of both drugs were detected in plasma at 6 hours with elimination at 24 hours. Presence of the two drugs did not affect the plasma pharmacokinetics of each other (A and B). Intratumoral concentrations of the two drugs were quantified by euthanizing the same mice at 24 hours (C and D). Despite disappearance of the drugs in the plasma at 24 hours, high concentrations were observed in the xenograft tumor tissue with unchanged pharmacokinetics in the presence of both drugs.

Figure 1

A

H9 48hr Concentrations	Excess over Bliss	72hr Concentrations	Excess over Bliss
0.002+0.02	14.3	0.002+0.02	7.4
0.002+0.5	14	0.002+0.5	6.1
0.002+0.248	13.2	0.002+0.248	5.4
0.002+1	12.5	0.002+1	4.9

B

HH, 48hr Concentrations	Excess over Bliss	72hr Concentrations	Excess over Bliss
0.002+0.02	-11.9	0.002+0.02	23.7
0.002+0.5	.11	0.002+0.5	21.1
0.002+0.248	8.5	0.002+0.248	23.2
0.002+1	-1.8	0.002+1	25.4

C

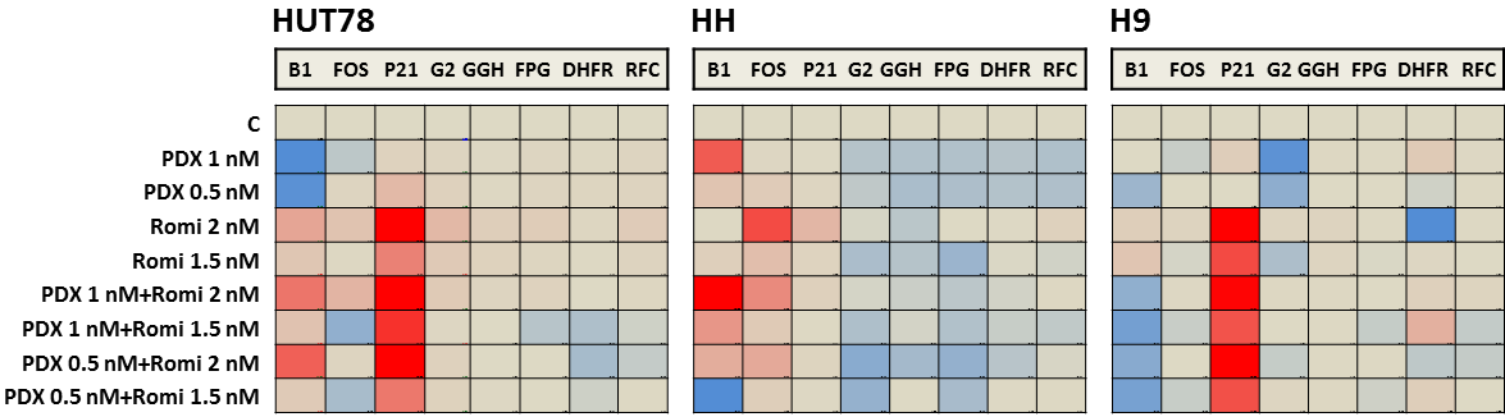

Figure 2

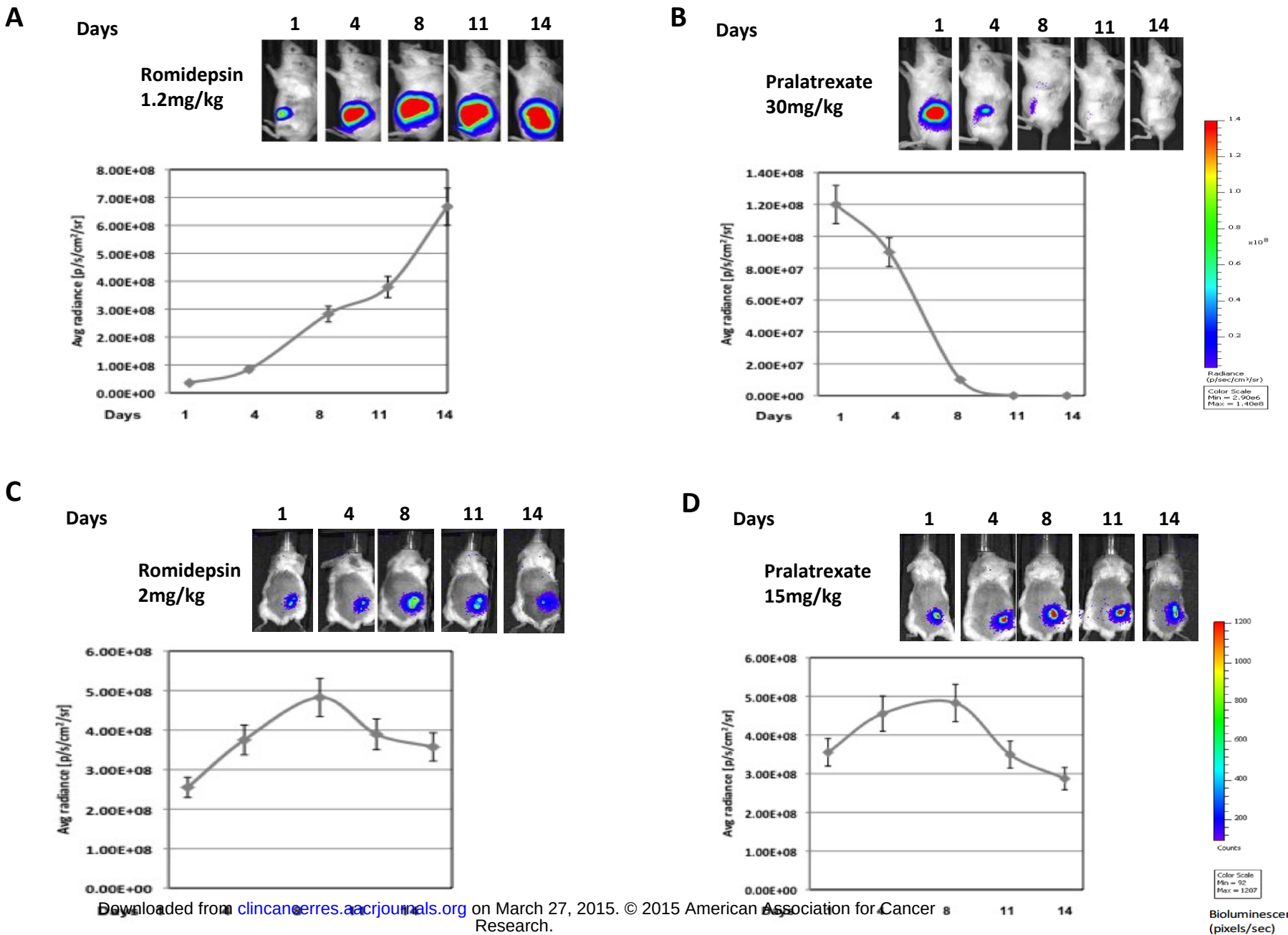

Figure 3

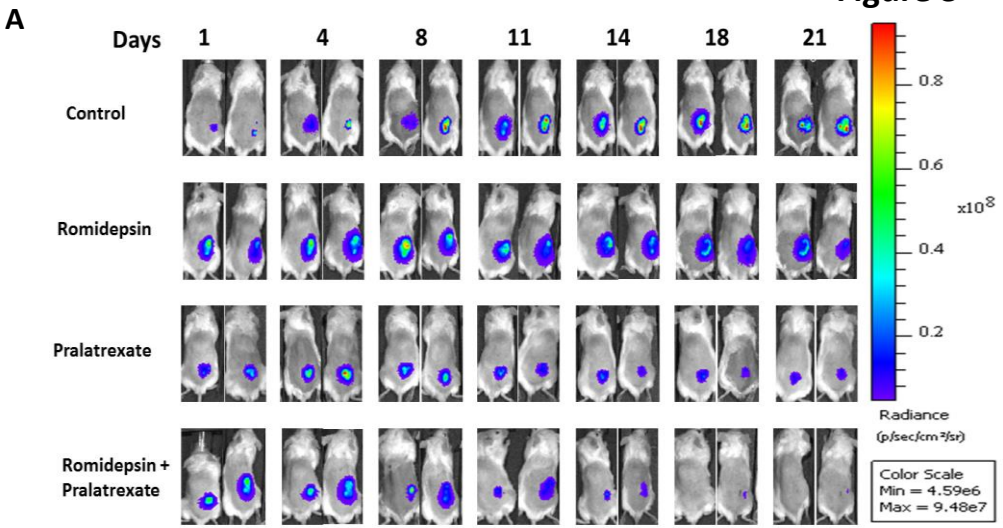

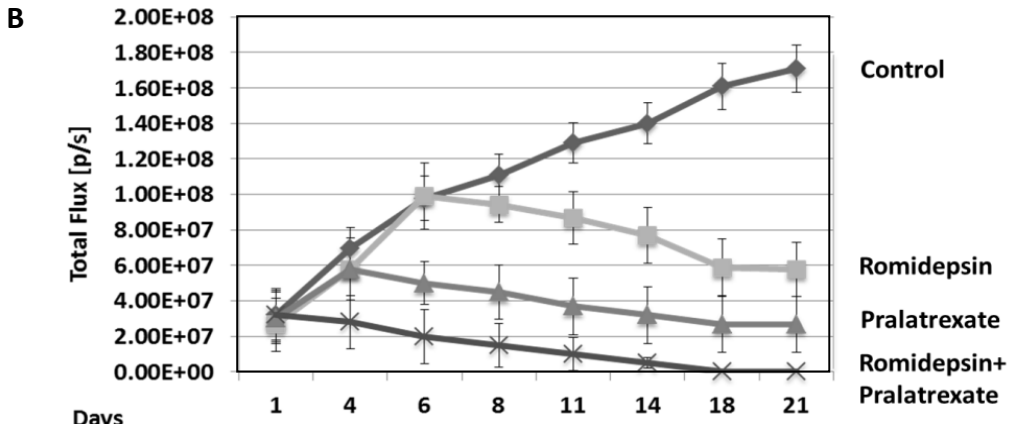

Treatment group	Estimated log-intensity (p-value)			
	4th day	6th day	11th day	18th day
Control	7.82	7.88	8.04	8.27
Romidepsin	7.76 (0.002)	7.77 (0.002)	7.81 (0.002)	7.85 (0.002)
Pralatrexate	7.65 (0.003)	7.62 (0.003)	7.55 (0.003)	7.46 (0.003)
Romidepsin + Pralatrexate	7.41 (0.002)	7.30 (0.002)	7.04 (0.002)	6.67 (0.002)

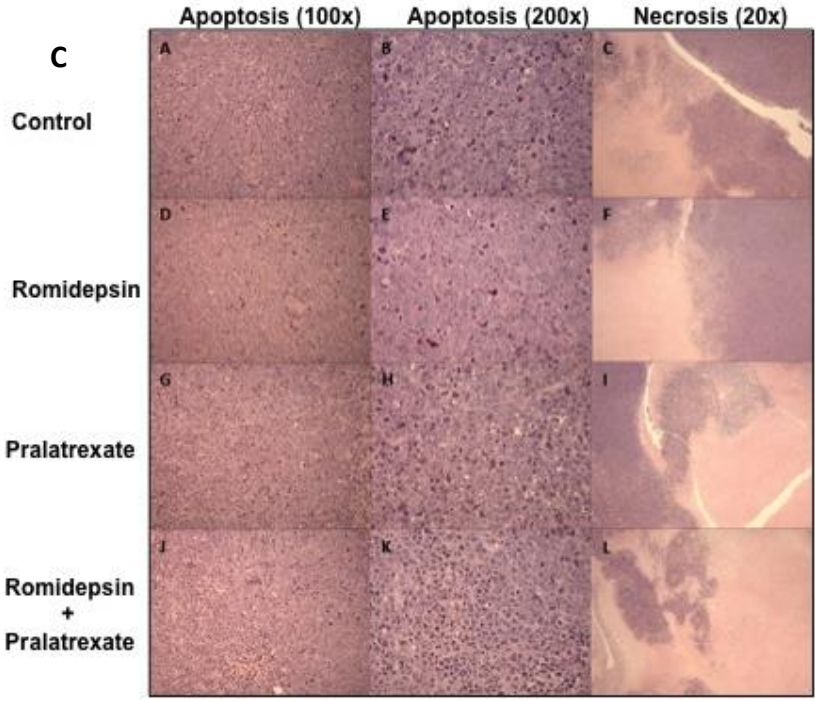

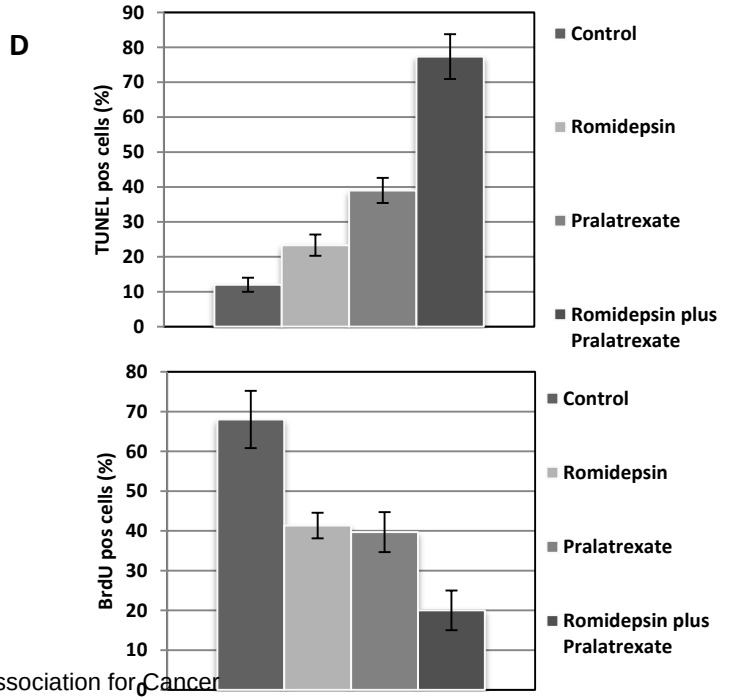

Figure 4

A

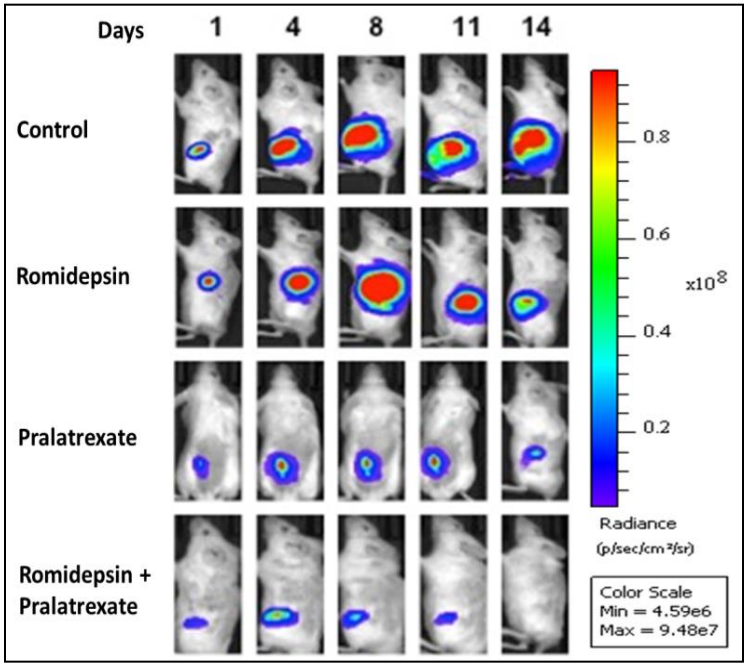

C

Treatment group	Estimated log-intensity (p-value)			
	4th day	8th day	11th day	14th day
Control	7.78 (<0.05)	8.09 (<0.05)	8.32 (<0.05)	8.55 (<0.05)
Romidepsin	7.75 (<0.05)	8.00 (<0.05)	8.20 (<0.05)	8.39 (<0.05)
Pralatrexate	7.58 (0.02)	7.74 (<0.05)	7.86 (<0.05)	7.98 (<0.05)
Romidepsin + Pralatrexate	7.49	7.24	7.06	6.87

B

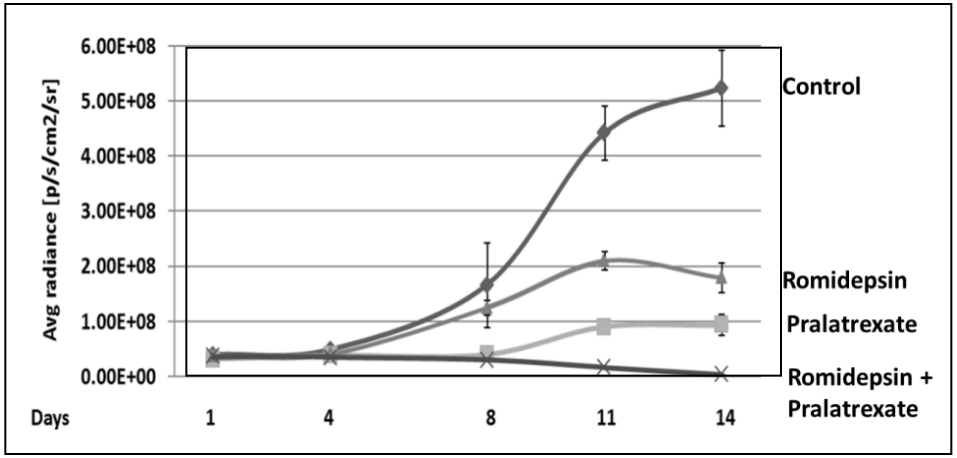

Figure 5

A

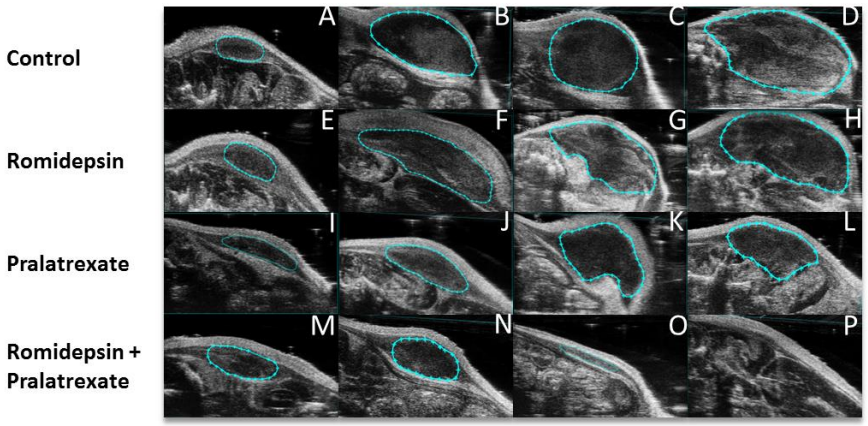

C

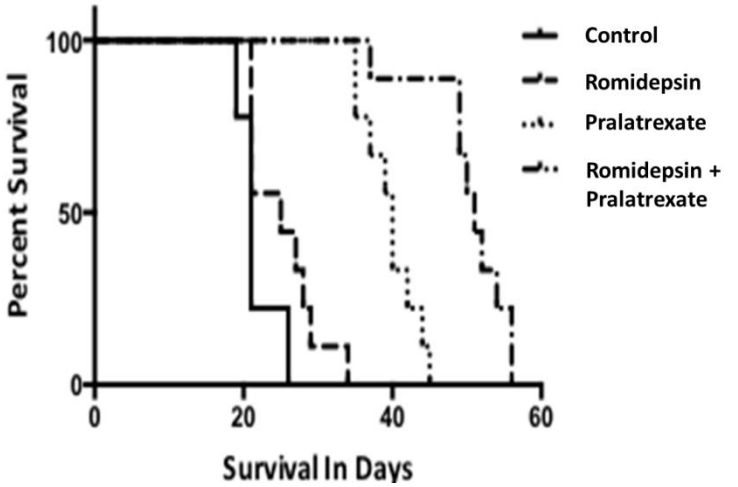

B

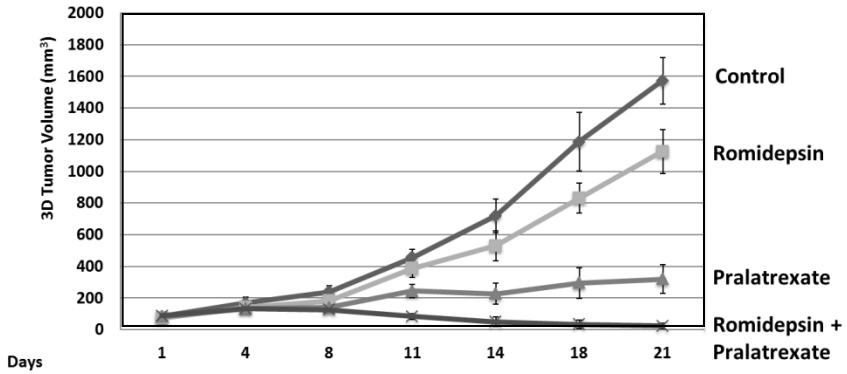

Treatment group	Estimated log-volume (p-value)			
	4th day	6th day	11th day	18th day
Control	2.16	2.29	2.61	3.06
Romidepsin	2.14 (0.48)	2.25 (0.1)	2.53 (0.004)	2.92 (<0.05)
Pralatrexate	2.08 (0.012)	2.14 (<0.05)	2.27 (<0.05)	2.46 (<0.05)
Romidepsin + Pralatrexate	2.06 (0.002)	1.96 (<0.05)	1.72 (<0.05)	1.39 (<0.05)

D

Treatment group	Median survival time (in days)	95% Confidence Interval		P-value from the Log-rank test
		Lower	Upper	
Control	21	19	26	Reference
Romidepsin	25	21	29	0.0002
Pralatrexate	40	35	44	<0.0001
Romidepsin + Pralatrexate	51	37	56	<0.0001

Figure 6

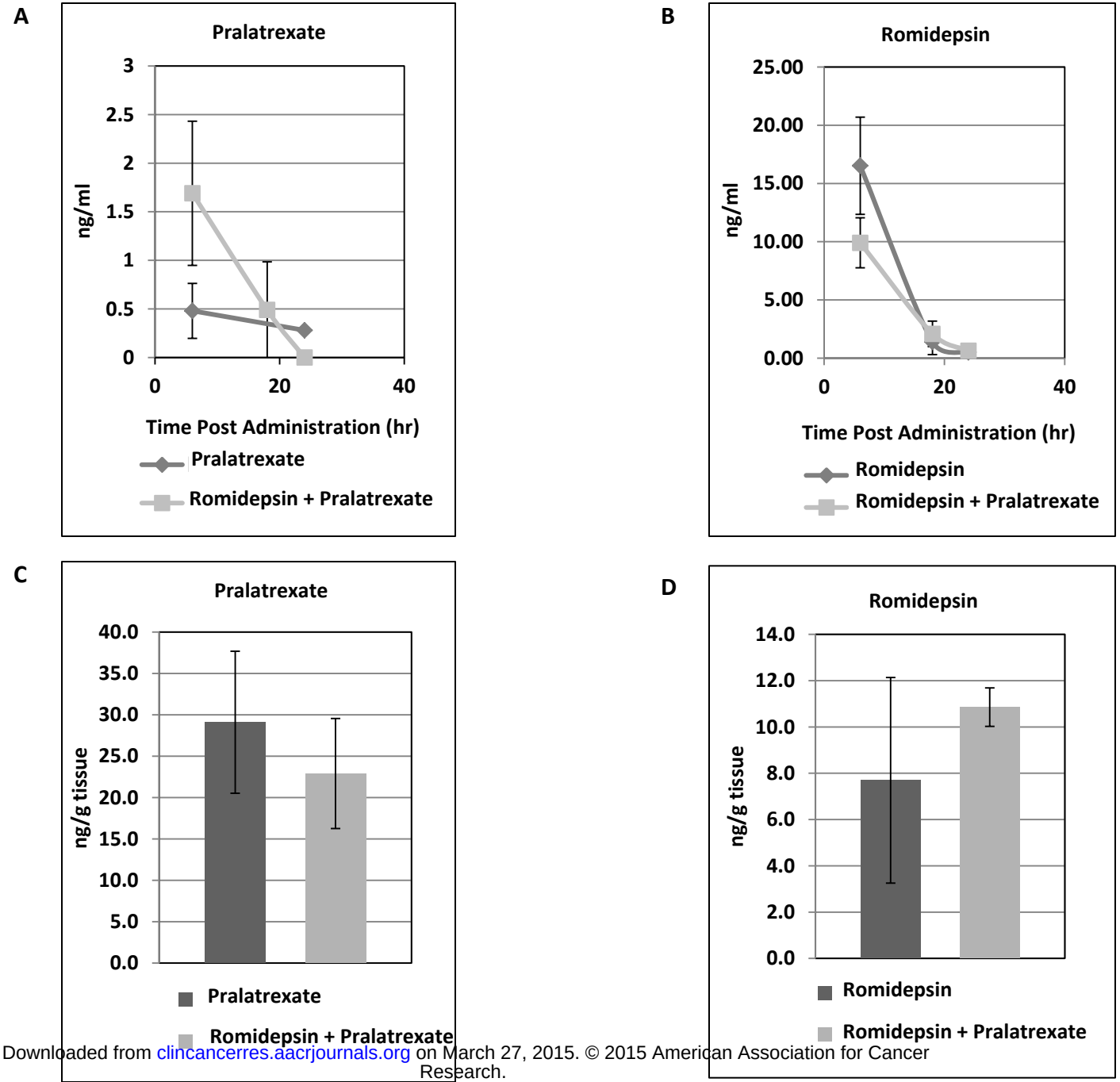

AACR American Association for Cancer Research

Clinical Cancer Research

Preclinical Pharmacologic Evaluation of Pralatrexate and Romidepsin Confirms Potent Synergy of the Combination in a Murine Model of Human T-cell Lymphoma

Salvia Jain, Xavier Jirau-Serrano, Kelly M Zullo, et al.

Clin Cancer Res Published OnlineFirst February 12, 2015.